

with corresponding decreases in the hole diameter of the capillary, this system can be applied to image a wide variety of objects in various fields including medical radiography.

## 6. Summary

In summary, we developed a conventional quasi-monochromatic parallel radiography system utilizing a polycapillary plate with a hole diameter of 25  $\mu\text{m}$  and a CR system. Quasi-monochromatic characteristic X-rays were obtained by a 10  $\mu\text{m}$ -thick copper filter with a tube voltage of 20 kV. The X-rays from the tube were formed into parallel beams in order to perform radiography. The image dimension increased slightly with corresponding increases in the distance between the radiographic object and the imaging plate, and we observed a 50  $\mu\text{m}$  tungsten wire and fine blood vessels clearly.

## Acknowledgements

This work was supported by Grants-in-Aid for Scientific Research and Advanced Medical Scientific Research from MECSST (12670902, 13470154, and 13877114), Grants from Keiryō Research Foundation, JST (Test of Fostering Potential), NEDO, and MHLW (HLSRG, RAMT-nano-001, RHGTEFB-genome-005, and RGCD13C-1).

## References

- [1] E. Sato, S. Kimura, S. Kawasaki, H. Isobe, K. Takahashi, Y. Tamakawa, T. Yanagisawa, *Rev. Sci. Instrum.* 61 (1990) 2343.
- [2] E. Sato, A. Shikoda, S. Kimura, M. Sagae, T. Oizumi, K. Takahashi, Y. Hayasi, T. Shoji, K. Shishido, Y. Tamakawa, T. Yanagisawa, *SPIE* 1801 (1992) 628.
- [3] E. Sato, M. Sagae, K. Takahashi, T. Oizumi, H. Ojima, K. Takayama, Y. Tamakawa, T. Yanagisawa, A. Fujiwara, K. Mitoya, *SPIE* 2513 (1994) 649.
- [4] E. Sato, M. Sagae, K. Takahashi, A. Shikoda, T. Oizumi, H. Ojima, K. Takayama, Y. Tamakawa, T. Yanagisawa, A. Fujiwara, K. Mitoya, *SPIE* 2513 (1994) 723.
- [5] A. Shikoda, E. Sato, M. Sagae, T. Oizumi, Y. Tamakawa, T. Yanagisawa, *Rev. Sci. Instrum.* 65 (1994) 850.
- [6] E. Sato, K. Takahashi, M. Sagae, S. Kimura, T. Oizumi, Y. Hayasi, Y. Tamakawa, T. Yanagisawa, *Med. Biol. Eng. Comput.* 32 (1994) 289.
- [7] K. Takahashi, E. Sato, M. Sagae, T. Oizumi, Y. Tamakawa, T. Yanagisawa, *Jpn. J. Appl. Phys.* 33 (1994) 4146.
- [8] E. Sato, M. Sagae, A. Shikoda, K. Takahashi, T. Oizumi, M. Yamamoto, A. Takabe, K. Sakamaki, Y. Hayasi, H. Ojima, K. Takayama, Y. Tamakawa, *SPIE* 2869 (1996) 937.
- [9] E. Sato, R. Germer, Y. Hayasi, E. Tanaka, H. Mori, T. Kawai, T. Usuki, K. Sato, H. Obara, M. Zuguchi, T. Ichimaru, H. Ojima, K. Takayama, H. Ido, *SPIE* 4948 (2002) 604.
- [10] E. Sato, Y. Hayasi, R. Germer, E. Tanaka, H. Mori, T. Kawai, H. Obara, T. Ichimaru, K. Takayama, H. Ido, *Jpn. J. Med. Imag. Inform. Sci.* 20 (2003) 148.
- [11] E. Sato, Y. Hayasi, R. Germer, E. Tanaka, H. Mori, T. Kawai, H. Obara, T. Ichimaru, K. Takayama, H. Ido, *Jpn. J. Med. Phys.* 20 (2003) 123.
- [12] H. Mori, K. Hyodo, E. Tanaka, M.U. Mohammed, A. Yamakawa, Y. Shinozaki, H. Nakazawa, Y. Tanaka, T. Sekka, Y. Iwata, S. Honda, K. Umetani, H. Ueki, T. Yokoyama, K. Tanioka, M. Kubota, H. Hosaka, N. Ishizawa, M. Ando, *Radiology* 201 (1996) 173.
- [13] T.J. Davis, D. Gao, T.E. Gureyev, A.W. Stevenson, S.W. Wilkims, *Nature* 373 (1995) 595.
- [14] A. Momose, T. Takeda, Y. Itai, K. Hirano, *Nat. Med.* 2 (4) (1996) 473.
- [15] A. Ishisaka, H. Ohara, C. Honda, *Opt. Rev.* 7 (2000) 566.
- [16] A.A. Bzhanmikov, N. Langhoff, J. Schmalz, R. Wedell, V.L. Beloglazov, N.F. Lebedev, *SPIE* 3444 (1998) 430.
- [17] Q.F. Xiao, S.V. Poturaef, *Nucl. Instr. Meth. Phys. Res. A* 347 (1994) 376.
- [18] E. Sato, Y. Hayasi, E. Tanaka, H. Mori, T. Kawai, H. Obara, T. Ichimaru, K. Takayama, H. Ido, T. Usuki, K. Sato, Y. Tamakawa, *SPIE* 4508 (2001) 176.
- [19] E. Sato, H. Toriyabe, Y. Hayasi, E. Tanaka, H. Mori, T. Kawai, T. Usuki, K. Sato, H. Obara, T. Ichimaru, K. Takayama, H. Ido, Y. Tamakawa, *SPIE* 4682 (2002) 298.
- [20] E. Sato, Y. Hayasi, T. Usuki, K. Sato, H. Ojima, K. Takayama, H. Ido, in: *Proceedings of the 3rd Korea-Japan Joint Meeting on Medical Physics*, Gyeongju, 2002, p. 400.
- [21] E. Sato, K. Sato, Y. Tamakawa, *Ann. Rep. Iwate Med. Univ. Sch. Lib. Arts Sci.* 35 (2000) 13.

## Quasi-monochromatic polycapillary imaging utilizing a computed radiography system

Eiichi Sato<sup>a</sup>, Yasuomi Hayasi<sup>a</sup>, Etsuro Tanaka<sup>b</sup>, Hidezo Mori<sup>c</sup>, Toshiaki Kawai<sup>d</sup>, Toshio Ichimaru<sup>e</sup>,  
Fumiko Obata<sup>f</sup>, Kiyomi Takahashi<sup>f</sup>, Sigehiro Sato<sup>f</sup>, Kazuyoshi Takayama<sup>g</sup> and Hideaki Ido<sup>h</sup>

<sup>a</sup>Department of Physics, Iwate Medical University, 3-16-1 Honchodori, Morioka 020-0015, Japan

<sup>b</sup>Department of Nutritional Science, Faculty of Applied Bio-science, Tokyo University of  
Agriculture, 1-1-1 Sakuragaoka, Setagaya-ku 156-8502, Japan

<sup>c</sup>Department of Cardiac Physiology, National Cardiovascular Center Research Institute, 5-7-1  
Fujishiro-dai, Suita, Osaka 565-8565, Japan

<sup>d</sup>Electron Tube Division #2, Hamamatsu Photonics Inc., 314-5 Shimokanzo, Toyooka Village,  
Iwata-gun 438-0193, Japan

<sup>e</sup>Department of Radiological Technology, School of Health Sciences, Hirosaki University, 66-1  
Honcho, Hirosaki 036-8564, Japan

<sup>f</sup>Department of Microbiology, School of Medicine, Iwate Medical University, 19-1 Uchimarui,  
Morioka 020-8505, Japan

<sup>g</sup>Shock Wave Research Center, Institute of Fluid Science, Tohoku University, 2-1-1 Katahira,  
Aoba-ku, Sendai 980-8577, Japan

<sup>h</sup>Department of Applied Physics, Faculty of Engineering, Tohoku Gakuin University, 1-13-1  
Chuo, Tagajo 985-8537, Japan

### ABSTRACT

A fundamental study on quasi-monochromatic parallel radiography using a polycapillary plate and a copper-target x-ray tube is described. The x-ray generator consists of a negative high-voltage power supply, a filament (hot cathode) power supply, and an x-ray tube. The negative high-voltage is applied to the cathode electrode, and the anode electrode is connected to the ground. In this experiment, the tube voltage was regulated from 12 to 22 kV, and the tube current was regulated within 3.0 mA by the filament temperature. The exposure time was controlled in order to obtain optimum x-ray intensity, and the maximum focal spot dimensions were approximately  $2.0 \times 1.5$  mm. The polycapillary plate was J5022-16 (Hamamatsu Photonics Inc.), and the plate thickness was 1.0 mm. The outer, effective, and hole diameters were 33 mm, 27 mm, and 10  $\mu\text{m}$ , respectively. Quasi-monochromatic x-rays were produced using a 10  $\mu\text{m}$ -thick copper filter with a tube voltage of 17 kV, and these rays were formed into parallel beams by the polycapillary. The radiogram was taken using a computed radiography system utilizing imaging plates. In the measurement of image resolution, the resolution hardly varied according to increases in the distance between the chart and imaging plate using a polycapillary. We could observe a 50  $\mu\text{m}$  tungsten wire clearly, and fine blood vessels of approximately 100  $\mu\text{m}$  were visible in angiography.

**Keywords:** Parallel radiography, quasi-monochromatic x-ray, characteristic x-ray, x-ray lens, polycapillary plate

## 1. INTRODUCTION

Monochromatic parallel x-ray beams are typically produced by a synchrotron in conjunction with single crystals and have been applied in high contrast micro-angiography<sup>1</sup> and x-ray phase imaging.<sup>2-4</sup> In order to produce quasi-monochromatic x-rays without using the synchrotron, we developed a transmission type molybdenum x-ray tube.<sup>5</sup> Subsequently, flash x-ray tubes are employed to primarily perform high speed radiographies with biomedical applications. In particular, plasma flash x-ray tubes are very useful to produce intense and sharp characteristic x-rays<sup>6-11</sup> such as lasers.

With recent advances in x-ray optics, several different x-ray lenses<sup>12,13</sup> have been developed, and a polycapillary plate<sup>5,8,14</sup> has been shown to be useful to realize a low-priced x-ray system and to perform parallel radiography. Therefore, we performed parallel radiography using a tungsten-target x-ray tube and an x-ray film because the film is conventional and is useful to obtain a high image resolution.

In biomedical radiography, because both the brightness and the contrast of radiograms can be controlled by a Computed Radiography (CR) system<sup>15</sup> utilizing imaging plates, the CR system is useful to perform quasi-monochromatic parallel radiography, regardless of whether the image resolution falls. Therefore, in conjunction with the CR, we have to measure the fundamental characteristics of the polycapillary radiography.

In this paper, we describe a quasi-monochromatic parallel radiography system utilizing a fine polycapillary plate with a hole diameter of 10  $\mu\text{m}$ , a CR system, and a copper-target radiation tube in order to create a conventional x-ray system to be used instead of the synchrotron.

## 2. EXPERIMENTAL SETUP

Figure 1 shows the circuit diagram of the x-ray generator, which consists of a negative high-voltage power supply, a filament (hot cathode) power supply, and a copper-target x-ray tube. The negative high-voltage is applied to the cathode electrode, and the anode (target) is connected to the ground. In this experiment, the tube voltage was regulated from 12 to 22 kV, and the tube current was regulated by the filament temperature and ranged from 1.0 to 3.0 mA. The exposure time was controlled in order to obtain optimum x-ray intensity.

The experimental setup for performing parallel radiography is shown in Fig. 2. Quasi-monochromatic x-rays are produced using a 10  $\mu\text{m}$ -thick copper filter, and these rays are formed into parallel beams by a polycapillary plate (Fig. 3). The polycapillary is J5022-16 (Hamamatsu Photonics Inc.), and the thickness and the hole diameter of the polycapillary are 1.0 mm and 10  $\mu\text{m}$ , respectively. Radiography was performed by a CR system (Konica Regius 150) utilizing imaging plates.

The distance between the x-ray source and the polycapillary was 1.08 m, and the polycapillary plate was set on the aluminum plate. The distance between the polycapillary and imaging plates was regulated by the height of polymethyl methacrylate (PMMA) spacers of 30 mm in height. At a constant distance between the polycapillary and the imaging plate, the distance between the imaging plate and the chart was regulated by pipe-shaped brass spacers of 30 and 60 mm in height.

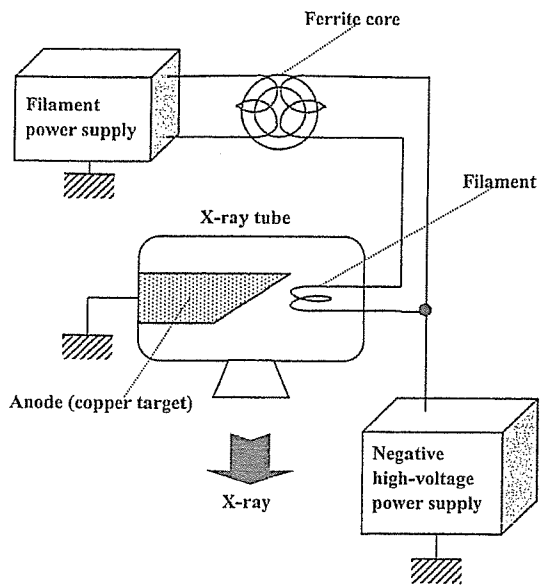


Figure 1: Circuit diagram of the x-ray generator.

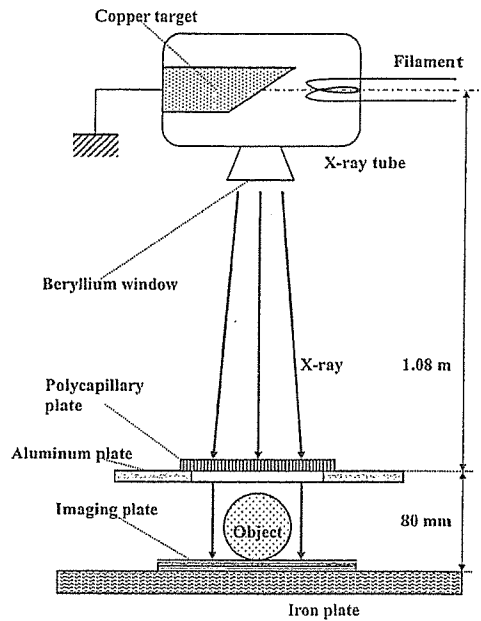
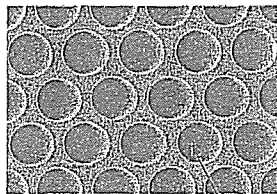


Figure 2: Experimental setup for parallel radiography utilizing a polycapillary plate and a CR system.



Capillary

Figure 3: Polycapillary plate.

### 3. CHARACTERISTICS

#### 3.1 Focal spot

In order to measure images of the x-ray source, we employed a pinhole camera with a hole diameter of  $50 \mu\text{m}$  (Fig. 4). When the tube voltage was increased, the spot intensity increased, and spot dimensions increased slightly and had values of approximately  $2.0 \times 1.5 \text{ mm}$ .

#### 3.2 X-ray spectra

X-ray spectra from the copper-target tube were measured by a transmission-type spectrometer with a lithium fluoride curved crystal  $0.5 \text{ mm}$  in thickness (Fig. 5). The spectra were taken by the CR system with a wide dynamic range, and relative x-ray intensity was calculated from Dicom digital data. Figure 6 shows measured spectra from the

copper target. When the tube voltage was increased, the bremsstrahlung x-ray intensity increased, and the characteristic x-ray intensity of  $K_{\alpha}$  and  $K_{\beta}$  lines also increased. Following insertion of the copper filter, the bremsstrahlung x-rays with energies higher than the K-absorption edge were absorbed effectively.

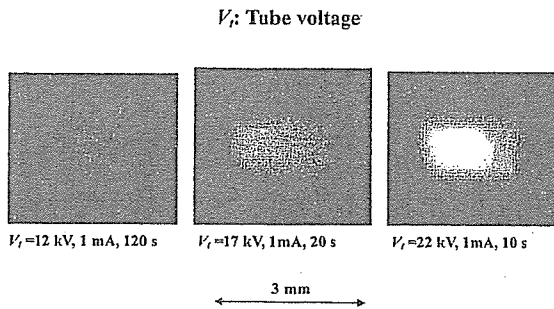


Figure 4: Images of the x-ray source measured by a 50  $\mu\text{m}$ -diameter pinhole with changes in the tube voltage.

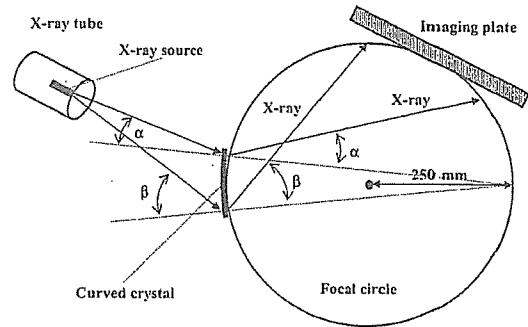


Figure 5: Transmission-type spectrometer with a lithium fluoride curved crystal and an imaging plate.

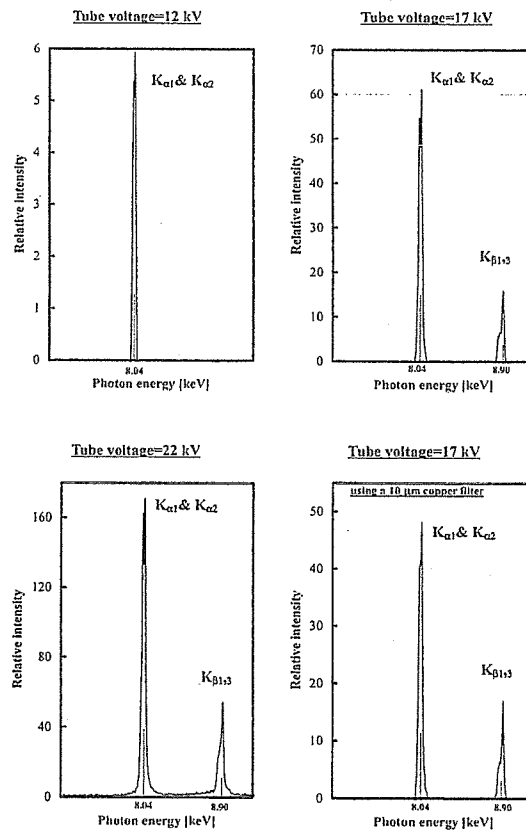


Figure 6: Measured x-ray spectra according to changes in the tube voltage.

#### 4. RADIOGRAPHY

The quasi-monochromatic radiography was performed with a tube voltage of 17 kV using the filter. Figure 7 shows radiography for imaging a polycapillary plate, and the radiograms of the polycapillary are shown in Fig. 8. The center of the black spot in the polycapillary radiogram was mainly imaged by direct transmission beams through capillary holes. As shown in this figure, the spot dimensions increased slightly according to decreases in the PMMA spacer height.

Figure 9 shows the parallel radiography for imaging a test chart, and the polycapillary was set on the aluminum plate. In this radiography, when the spacer height was increased, the image resolution hardly varied, and the image dimensions decreased slightly (Fig. 10). Next, when the height of the brass spacer was decreased, the image resolution hardly varied, and the dimensions again decreased slightly (Figs. 11 and 12).

Figures 13 and 14 show radiography and the radiogram of tungsten wires on a PMMA spacer, respectively. Although the image contrast increased with increases in the wire diameter, a 50  $\mu\text{m}$ -diameter wire could be observed. An angiography of a rabbit heart is shown in Fig. 15; iodine-based microspheres of 20  $\mu\text{m}$  diameter were used, and fine blood vessels of about 50  $\mu\text{m}$  were visible (Fig. 16).

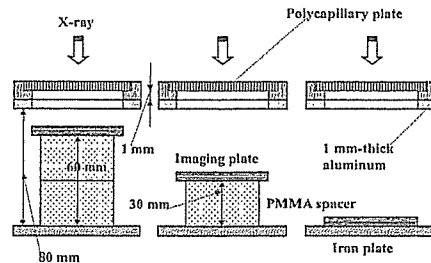


Figure 7: Radiography for imaging a polycapillary plate according to changes in the distance between the polycapillary and imaging plates.

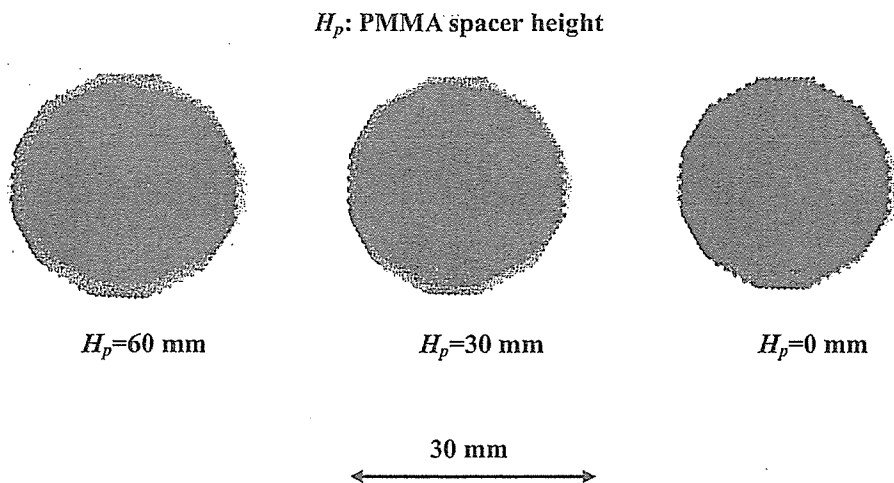


Figure 8: Radiograms of a polycapillary plate according to changes in the PMMA height.

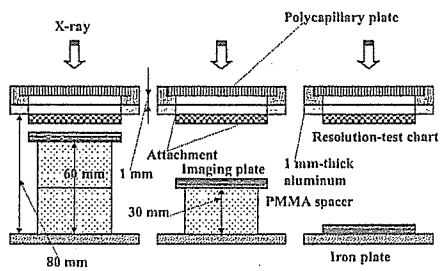


Figure 9: Radiography for imaging a test chart using a polycapillary plate according to the PMMA height.

$H_p$ : PMMA spacer height

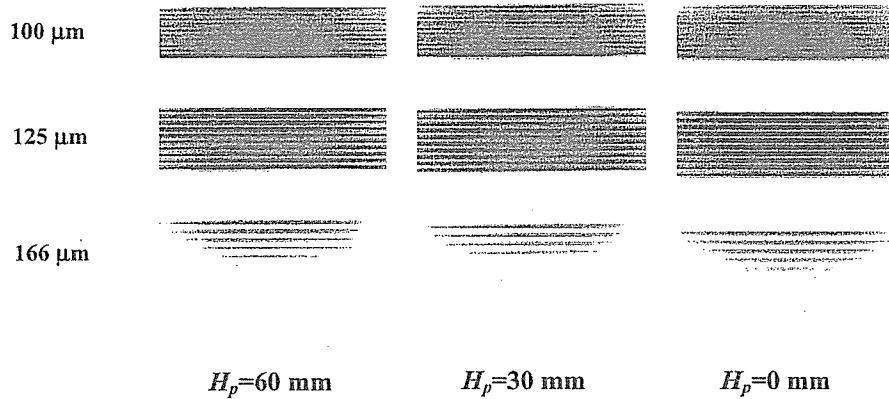


Figure 10: Radiograms of a test chart using a polycapillary plate according to the PMMA height.

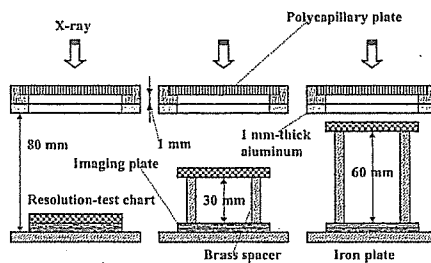


Figure 11: Radiography for imaging a test chart using a polycapillary plate according to the brass spacer height.

$H_b$ : Brass spacer height

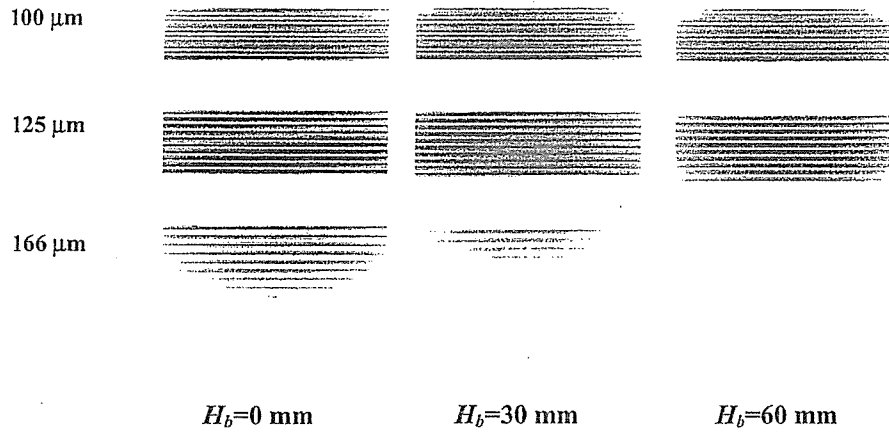


Figure 12: Radiograms of a test chart using the polycapillary according to the brass spacer height.

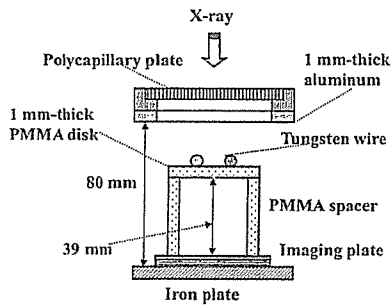


Figure 13: Radiography for imaging tungsten wires using the polycapillary.

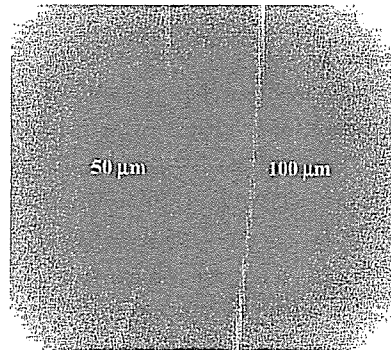


Figure 14: Radiograms of tungsten wires on a PMMA spacer.



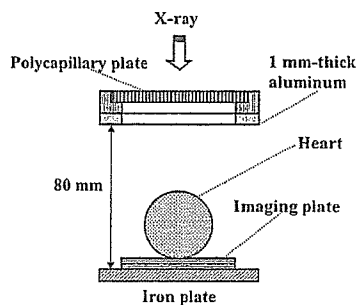


Figure 15: Parallel angiography of a heart extracted from a rabbit using iodine-based microspheres.

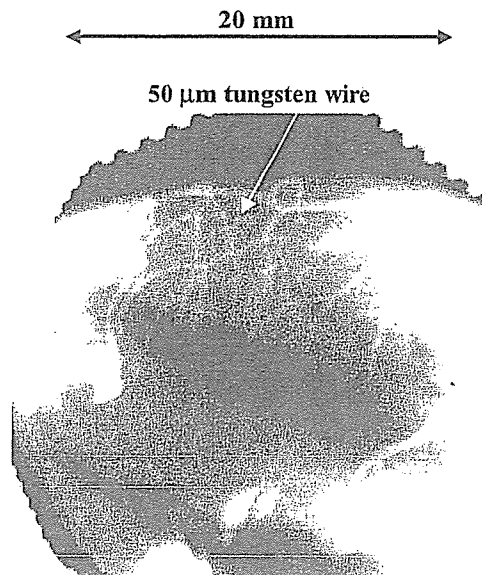


Figure 16: Angiogram of the heart using the polycapillary.

## 5. DISCUSSION

In this research, we performed parallel radiography achieved with a polycapillary plate in conjunction with quasi-monochromatic x-rays, and obtained slightly higher image resolutions as compared with those obtained without using the plate. Currently, the image resolution of the polycapillary is primarily determined by the diameter of the capillary hole and the thickness, and is improved with decreases in the diameter and increases in the thickness. In cases where the CR system is employed, although the resolution of the CR system is primarily determined by the minimum sampling pitch of  $87.5 \mu\text{m}$ , we could observe  $50 \mu\text{m}$  tungsten wires easily.

The photon energies of the characteristic x-rays are determined by the target element, and the capillary thickness should be increased according to increases in the photon energy because the transmission intensity through capillary glass increases. Subsequently, in order to increase the parallelity for phase imaging, single crystals should be employed after passing through the polycapillary.

Because it is possible to increase the irradiation field by increasing the distance between the x-ray source and the polycapillary, this system can be applied to image a wide variety of objects in various fields, including medical radiography.

## ACKNOWLEDGMENTS

This work was supported by Grants-in-Aid for Scientific Research (12670902, 13470154, and 13877114) and Advanced Medical Scientific Research from MECSST, Grants from Keiryō Research Foundation, JST (Test of Fostering Potential), NEDO, and MHLW (HLSRG, RAMT-nano-001, RHGTEFB-genome-005, and RGCD13C-1).

## REFERENCES

1. H. Mori, K. Hyodo, E. Tanaka, M.U. Mohammed, A. Yamakawa, Y. Shinozaki, H. Nakazawa, Y. Tanaka, T. Sekka, Y. Iwata, S. Honda, K. Umetani, H. Ueki, T. Yokoyama, K. Tanioka, M. Kubota, H. Hosaka, N. Ishizawa and M. Ando, "Small-vessel radiography in situ with monochromatic synchrotron radiation," *Radiology*, **201**, pp. 173-177, 1996.
2. T.J. Davis, D. Gao, T.E. Gureyev, A.W. Stevenson and S.W. Wilkins, "Phase-contrast imaging of weakly absorbing materials using hard x-rays," *Nature*, **373**, pp. 595-597, 1995.
3. A. Momose, T. Takeda, Y. Itai and K. Hirano, "Phase-contrast x-ray computed tomography for observing biological soft tissues," *Nature Medicine*, **2(4)**, pp. 473-475, 1996.
4. A. Ishisaka, H. Ohara and C. Honda, "A new method of analyzing edge effect in phase contrast imaging with incoherent x-rays," *Opt. Rev.*, **7**, pp. 566-572, 2000.
5. E. Sato, M. Komatsu, Y. Hayasi, E. Tanaka, H. Mori, T. Kawai, T. Usuki, K. Sato, T. Ichimaru, K. Takayama and H. Ido, "Quasi-monochromatic parallel radiography achieved with a plane-focus x-ray tube," *SPIE*, **4786**, pp. 151-161, 2002.
6. E. Sato, Y. Hayasi, H. Mori, E. Tanaka, K. Takayama, H. Ido, K. Sakamaki and Y. Tamakawa, "Quasi-monochromatic x-ray production from the cerium target," *SPIE*, **4142**, pp. 17-28, 2000.
7. E. Sato, Y. Suzuki, Y. Hayashi, E. Tanaka, H. Mori, T. Kawai, K. Takayama, H. Ido and Y. Tamakawa, "High-intensity quasi-monochromatic x-ray irradiation from the linear plasma target," *SPIE*, **4505**, pp. 154-164, 2001.
8. E. Sato, Y. Hayashi, E. Tanaka, H. Mori, T. Kawai, H. Obara, T. Ichimaru, K. Takayama, H. Ido, T. Usuki, K. Sato and Y. Tamakawa, "Polycapillary radiography using a quasi-x-ray laser generator," *SPIE*, **4508**, pp. 176-187, 2001.
9. E. Sato, Y. Hayasi, E. Tanaka, H. Mori, T. Kawai, T. Usuki, K. Sato, H. Obara, T. Ichimaru, K. Takayama, H. Ido and Y. Tamakawa, "Quasi-monochromatic radiography using a high-intensity quasi-x-ray laser generator," *SPIE*, **4682**, pp. 538-548 2002.
10. E. Sato, Y. Hayasi, E. Tanaka, H. Mori, T. Kawai, K. Takayama and H. Ido, "Irradiation of intense characteristic x-rays from weakly ionized linear plasma," *Proc 3<sup>rd</sup> Korea-Japan Joint Meeting on Medical Physics, Gyeongju*, pp. 396-399, 2002.
11. E. Sato, Y. Hayasi, R. Germer, E. Tanaka, H. Mori, T. Kawai, H. Obara, T. Ichimaru, K. Takayama and H. Ido, "Intense characteristic x-ray irradiation from weakly ionized linear plasma and applications," *Jpn. J. Med. Imag. Inform. Sci.*, **20**, pp. 148-155, 2003.
12. Q.F. Xiao and S.V. Poturaef, "Polycapillary-based x-ray optics," *Nucl. Instr. Meth. Phys. Res. A*, **347**, pp. 376-383, 1994.
13. A.A. Bzhanmikov, N. Langhoff, J. Schmalz, R. Wedell, V.L. Beloglazov and N.F. Lebedev, "Polycapillary conic collimator for micro-XRF," *SPIE*, **3444**, pp. 430-435, 1998.
14. E. Sato, H. Toriyabe, Y. Hayasi, E. Tanaka, H. Mori, T. Kawai, T. Usuki, K. Sato, H. Obara, T. Ichimaru, K. Takayama, H. Ido and Y. Tamakawa, "Fundamental study on parallel beam radiography using a polycapillary plate," *SPIE*, **4682**, pp. 298-310, 2002.
15. E. Sato, K. Sato and Y. Tamakawa, "Film-less computed radiography system for high-speed Imaging," *Ann. Rep. Iwate Med. Univ. Sch. Lib. Arts and Sci.*, **35**, pp. 13-23, 2000.

# Extremely soft x-ray generator and its applications

Eiichi Sato<sup>\*a</sup>, Fumiko Obata<sup>b</sup>, Kiyomi Takahashi<sup>b</sup>, Shigehiro Sato<sup>b</sup>, Etsuro Tanaka<sup>c</sup>, Hidezo Mori<sup>d</sup>, Toshiaki Kawai<sup>e</sup>, Toshio Ichimaru<sup>f</sup>, Kazuyoshi Takayama<sup>g</sup> and Hideaki Ido<sup>h</sup>

<sup>a</sup> Department of Physics, Iwate Medical University, 3-16-1 Honchodori, Morioka 020-0015, Japan

<sup>b</sup> Department of Microbiology, School of Medicine, Iwate Medical University, 19-1 Uchimaru, Morioka 020-8505, Japan

<sup>c</sup> Department of Nutritional Science, Faculty of Applied Bio-science, Tokyo University of Agriculture, 1-1-1 Sakuragaoka, Setagaya-ku 156-8502, Japan

<sup>d</sup> Department of Cardiac Physiology, National Cardiovascular Center Research Institute, 5-7-1 Fujishirodai, Suita, Osaka 565-8565 Japan

<sup>e</sup> Electron Tube Division #2, Hamamatsu Photonics Inc., 314-5 Shimokanzo, Toyooka Village, Iwata-gun 438-0193, Japan

<sup>f</sup> Department of Radiological Technology, School of Health Sciences, Hirosaki University, 66-1 Honcho, Hirosaki 036-8564, Japan

<sup>g</sup> Shock Wave Research Center, Institute of Fluid Science, Tohoku University, 2-1-1 Katahira, Sendai 980-8577, Japan,

<sup>h</sup> Department of Applied Physics and Informatics, Faculty of Engineering, Tohoku Gakuin University, 1-13-1 Chuo, Tagajo 985-8537, Japan

## ABSTRACT

The development of an extremely soft x-ray generator with a tungsten-target tube and its applications to radiography and disinfection are described. This generator consists of a high-voltage power supply, a filament power supply, and an x-ray tube. Negative high voltages are applied to the cathode electrode in the x-ray tube, and the tube voltage and current are regulated by the input of a transformer and the filament voltage, respectively. The x-ray tube is a glass-enclosed double-focus diode with a tungsten target and a 0.2 mm-thick beryllium window. The maximum tube voltage and electric power were 60 kV and 400 W, respectively. The focal-spot sizes were 4×4 (large) and 1×1 mm (small), respectively. Extremely soft radiography was performed with a computed radiography system, and we observed fine blood vessels of about 100  $\mu\text{m}$  with high contrasts. Using this generator, we performed the disinfection achieved with extremely soft x rays.

**Keywords:** extremely soft x-ray, thin beryllium window, soft x-ray disinfection, soft radiography

## 1. INTRODUCTION

Synchrotrons generate high-dose-rate bremsstrahlung x rays with wide photon energy latitudes, and monochromatic x-ray beams have been produced using single crystals. These rays have been employed to perform K-edge angiography<sup>1-3</sup> and phase imaging.<sup>4,6</sup> However, it is difficult to increase the irradiation field, due to the parallel beam, or to obtain sufficient machine times for various research projects, including medical applications.

Conventional medical x-ray generators produce both bremsstrahlung and characteristic x rays, and quasi-monochromatic x rays have been produced using K-edge filters. In contrast, flash x-ray generators utilize cold-cathode tubes, and the generators<sup>7-13</sup> with photon energies of lower than 150 keV can be employed to perform biomedical radiography. In order to produce monochromatic x rays, plasma flash x-ray generators<sup>14-18</sup> are useful, since quite intense and sharp characteristic x rays such as lasers have been produced from weakly ionized linear plasmas.

In order to produce monochromatic parallel beams using a hot-cathode x-ray tube in conjunction with the crystals, high-dose-rate bremsstrahlung x rays are needed, and the x-ray photon energy is selected by Bragg's angle. Therefore,

the thickness of the x-ray window of the tube should be decreased as much as possible so as to increase the x-ray dose rate and to produce soft bremsstrahlung x rays. In addition, soft x rays are useful to image soft-tissue objects, including biomedical objects, and the rays may be used to perform disinfection of various fungi, including anthrax, because the x rays are absorbed easily by fungi.

In the present research, we developed an extremely soft x-ray generator with a tungsten-target tube, and used it to perform preliminary studies on extremely soft radiography and disinfection.

## 2. GENERATOR

Figure 1 shows the block diagram of the x-ray generator, which consists of a high-voltage power supply (Fig. 2), an x-ray tube unit (Fig. 3), and a filament power supply. The negative high voltage is applied to the cathode electrode, and the anode (target) is connected to the ground potential. The x-ray tube is a glass-enclosed diode with a tungsten target and a 0.2 mm-thick beryllium window. In this experiment, the peak tube voltage was regulated from 10 to 15 kV using an auto transformer, and the peak tube current was regulated within 15 mA by the filament voltage (temperature). The exposure time is controlled in order to obtain optimum x-ray intensity, and the x-ray tube is a double-focus type with focal-spot dimensions of approximately  $4 \times 4$  (large spot) and  $1 \times 1$  mm (small spot), respectively.

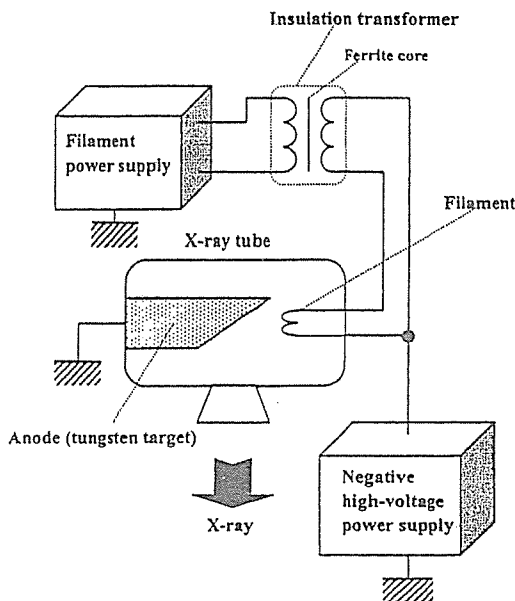


Fig. 1. Block diagram of extremely soft x-ray generator.

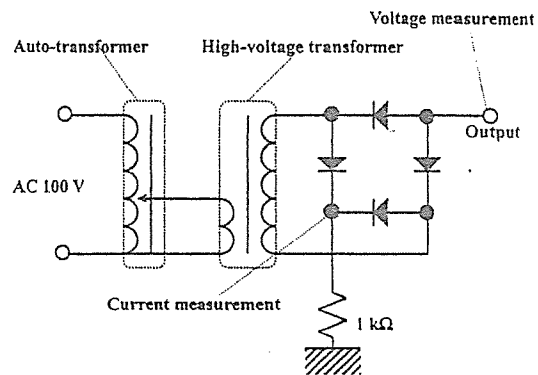


Fig. 2. Circuit diagram of high voltage power supply.

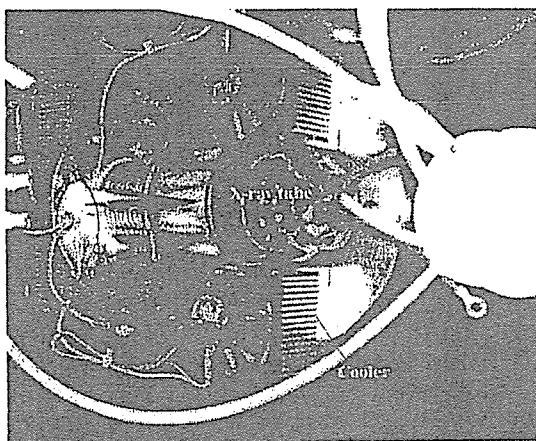


Fig. 3. X-ray tube unit with coolers.

### 3. CHARACTERISTICS

#### 3.1 Cathode voltage and current

The cathode voltage and current were measured by a high-voltage divider and a resistor, respectively, and the tube voltage was  $-1$  times the cathode voltage. Figure 4 shows variations in the voltage and current. The negative peak voltage increased when the input voltage from an auto transformer was increased. Next, the peak tube current was regulated constantly by the filament voltage.

#### 3.2 X-ray source

In order to measure images of the x-ray source, we employed a pinhole camera with a hole diameter of  $50 \mu\text{m}$  in conjunction with a Computed Radiography (CR) system.<sup>19</sup> The dimensions of small and large spots seldom varied and had values of approximately  $1 \times 1$  and  $4 \times 4 \text{mm}$ , respectively.

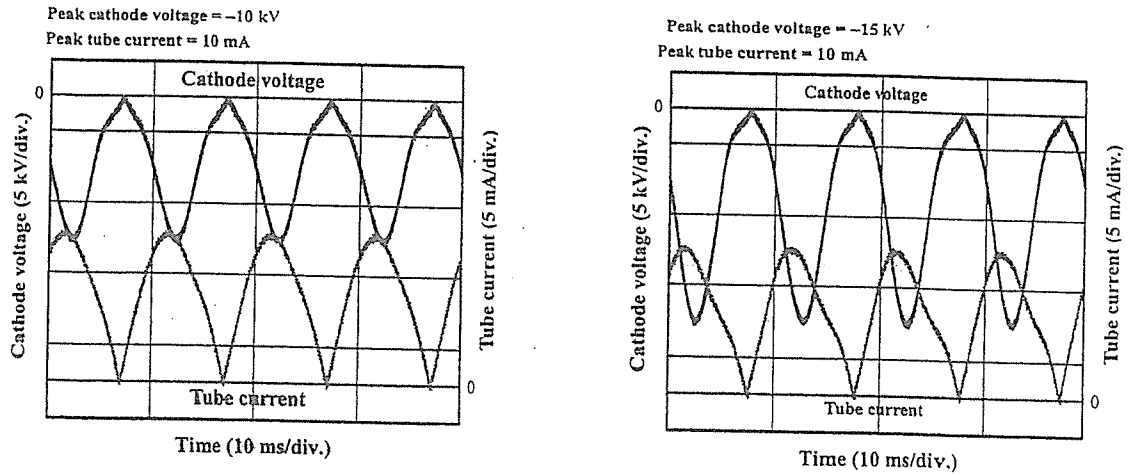


Fig. 4. Cathode voltages and tube currents at indicated conditions.

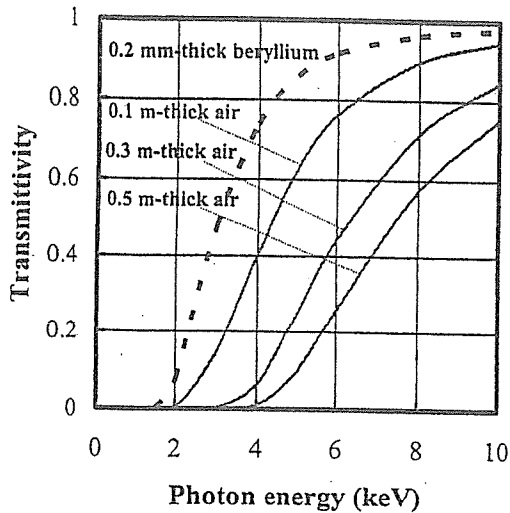


Fig. 5. Transmittivity of x rays with photon energy.

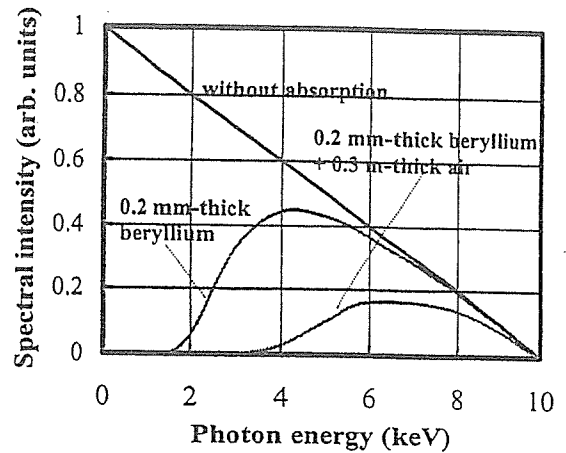


Fig. 6. Calculated bremsstrahlung spectra at indicated conditions.

### 3.3 X-ray spectra

Figure 5 shows transmittivity of beryllium and dry air with changes in the photon energy. When a 0.2 mm-thick beryllium window is employed, x-ray spectra with energies of lower than 2 keV are absorbed effectively. Subsequently, 0.5 m-thick air transmit x rays with energies of higher than 4 keV.

The bremsstrahlung x-ray spectra were calculated by the mass attenuation coefficients of the beryllium and the dry air at a constant tube voltage of 10 kV (Fig. 6). As shown in this figure, the soft x rays of lower than 2 keV were primarily absorbed by the beryllium x-ray window, and the rays were also absorbed by the air. Therefore, the distance should be decreased as much as possible in order to obtain soft x rays.

## 4. RADIOGRAPHY

The radiography was performed using the CR system (Konica Regius 150) and the small spot, and the distance between the x-ray source and imaging plate was 0.5 m. Next, the peak current ( $I_p$ ) and the exposure time were 10 mA and 10 s, respectively. Figure 7 shows radiograms of tungsten wires coiled around pipes made of polymethyl methacrylate with a peak tube voltage  $V_p$  of 15 kV. Although the image contrast increased with increases in the wire diameter, a 50  $\mu\text{m}$ -diameter wire could be observed.

A radiogram of a thin film for food wrapping is shown in Fig. 8. The  $V_p$  was 15 kV, and the image of a folded film is visible. Next, angiograms of rabbit hearts recorded using iodine microspheres of 15  $\mu\text{m}$  in diameter are shown in Fig. 9. These two images were obtained using a 1.0 mm-thick aluminum filter and without using the filter at a  $V_p$  of 15 kV. In the case where the filter was not employed, the coronary arteries were barely visible, since the heart did not transmit extremely soft x rays. Finally, Fig. 10 shows an angiogram of the external ear of a rabbit; iodine-based microspheres of 15  $\mu\text{m}$  in diameter were used at a  $V_p$  of 10 kV, and fine blood vessels of about 50  $\mu\text{m}$  were clearly visible.

## 5. DISINFECTION

Figure 11 shows the experimental setup for disinfection using soft x rays. Fungi were enclosed in an envelope and were exposed to soft x rays using the large spot, and we performed disinfection of three fungi with changes in the exposure time using a copper box with a  $V_p$  of 15 kV and an  $I_p$  of 10 mA. In these experiments, the complete disinfection times for *Bacillus subtilis* and *staphylococcus* were approximately 15 and 3 hours, respectively, and the time for *B-coli* was less than 1 hour (Tables 1-3).

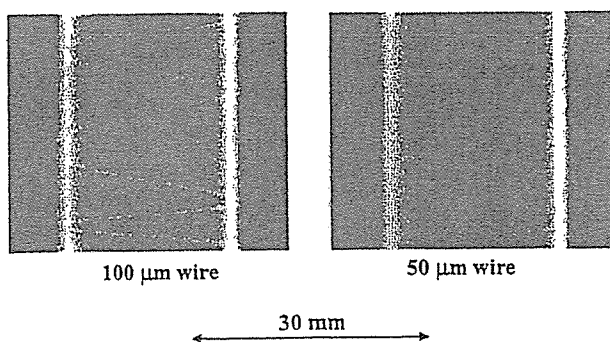


Fig. 7. Radiograms of tungsten wires of 50 and 100  $\mu\text{m}$  in diameter coiled around pipes made of polymethyl methacrylate.



Fig. 8. Radiogram of film.

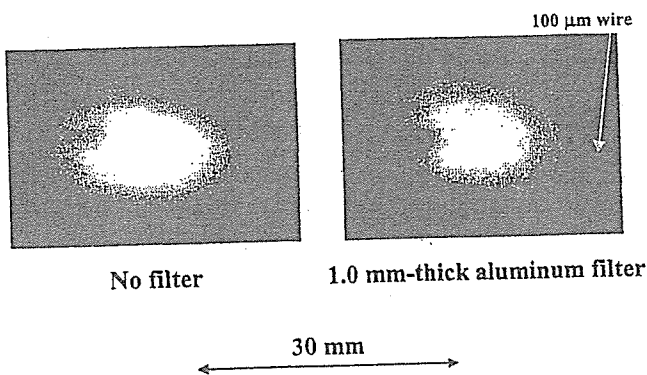


Fig. 9. Angiograms of rabbit hearts.

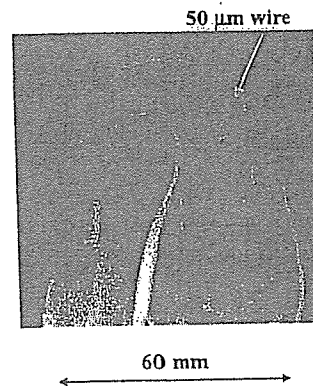


Fig. 10. Angiograms of external ear of rabbit.

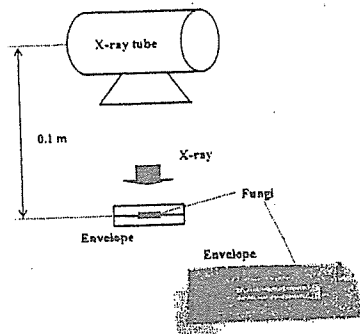


Fig. 11. Experimental setup for disinfection.

Table 1. Disinfection test for *Bacillus subtilis*.

Culture time (day) \ Exposure time (hour)	1	2	3	4
6	+	+	+	+
12	-	-	+	+
18	-	-	-	-
24	-	-	-	-

Table 2. Disinfection test for staphylococcus.

Culture time (day) \ Exposure time (hour)	1	2	3	4
1	-	+	+	+
2	-	+	+	+
3	-	-	-	-
4	-	-	-	-

Table 3. Disinfection test for *B-coli*.

Culture time (day) \ Exposure time (hour)	1	2	3	4
1	-	-	-	-
2	-	-	-	-
3	-	-	-	-
4	-	-	-	-

## 6. DISCUSSION

In the present work, we succeeded in generating extremely soft x rays using a 0.2 mm-thick beryllium window in conjunction with a tungsten target. By the calculation of bremsstrahlung x rays, x rays with energies higher than 2 keV are produced. However, it is very difficult to measure the x-ray dose because there are no dosimeters with constant energy sensitivities.

In radiography, the image quality hardened in response to increases in the thickness of the aluminum filter, because the low-photon-energy x rays of the spectra were absorbed easily by the filter. Using this x-ray generator, although K-series characteristic x rays of tungsten are not produced, due to the tube voltage, the photon energies of the characteristic x rays

can be selected by the target element.

In the disinfection, the distance between the x-ray source and fungi should be decreased as much as possible to decrease the absorbed x-ray dose by air. Subsequently, because the air is dissociated greatly, ion beams will also be a useful technique for the disinfection and the excluding of static electricity from semiconductor devices. Because it is possible to produce low-photon-energy x rays and to perform extremely soft radiography and x-ray disinfection, and to exclude electricity, this system can be applied in various fields.

## ACKNOWLEDGMENTS

This work was supported by Grants-in-Aid for Scientific Research (13470154, 13877114, and 16591222) and Advanced Medical Scientific Research from MECSSST, Health and Labor Sciences Research Grants (RAMT-nano-001, RHGTEFB-genome-005 and RHGTEFB-saisei-003), Grants from Keiryō Research Foundation, The Promotion and Mutual Aid Corporation for Private Schools of Japan, Japan Science and Technology Agency (JST), and New Energy and Industrial Technology Development Organization (NEDO, Industrial Technology Research Grant Program in '03).

## REFERENCES

1. A. C. Thompson, H. D. Zeman, G. S. Brown, J. Morrison, P. Reiser, V. Padmanabahn, L. Ong, S. Green, J. Giacomini, H. Gordon and E. Rubenstein, "First operation of the medical research facility at the NSLS for coronary angiography," *Rev. Sci. Instrum.*, **63**, pp. 625-628, 1992.
2. H. Mori, K. Hyodo, E. Tanaka, M. U. Mohammed, A. Yamakawa, Y. Shinozaki, H. Nakazawa, Y. Tanaka, T. Sekka, Y. Iwata, S. Honda, K. Umetani, H. Ueki, T. Yokoyama, K. Tanioka, M. Kubota, H. Hosaka, N. Ishizawa and M. Ando, "Small-vessel radiography in situ with monochromatic synchrotron radiation," *Radiology*, **201**, pp. 173-177, 1996.
3. K. Hyodo, M. Ando, Y. Oku, S. Yamamoto, T. Takeda, Y. Itai, S. Ohtsuka, Y. Sugishita and J. Tada, "Development of a two-dimensional imaging system for clinical applications of intravenous coronary angiography using intense synchrotron radiation produced by a multipole wiggler," *J. Synchrotron Rad.*, **5**, pp. 1123-1126, 1998.
4. T. J. Davis, D. Gao, T. E. Gureyev, A. W. Stevenson and S. W. Wilkims, "Phase-contrast imaging of weakly absorbing materials using hard x-rays," *Nature*, **373**, pp. 595-597, 1995.
5. A. Momose, T. Takeda, Y. Itai and K. Hirano, "Phase-contrast x-ray computed tomography for observing biological soft tissues," *Nature Medicine*, **2**, pp. 473-475, 1996.
6. M. Ando, A. Maksimenko, H. Sugiyama, W. Pattanasiriwisawa, K. Hyodo and C. Uyama, "A simple x-ray dark- and bright- field imaging using achromatic Laue optics," *Jpn. J. Appl. Phys.*, **41**, pp. L1016-L1018, 2002.
7. E. Sato, S. Kimura, S. Kawasaki, H. Isobe, K. Takahashi, Y. Tamakawa and T. Yanagisawa, "Repetitive flash x-ray generator utilizing a simple diode with a new type of energy-selective function," *Rev. Sci. Instrum.*, **61**, pp. 2343-2348, 1990.
8. E. Sato, M. Sagae, K. Takahashi, T. Oizumi, H. Ojima, K. Takayama, Y. Tamakawa, T. Yanagisawa, A. Fujiwara and K. Mitoya, "High-speed soft x-ray generators in biomedicine," *SPIE*, **2513**, pp. 649-667, 1994.
9. E. Sato, M. Sagae, K. Takahashi, A. Shikoda, T. Oizumi, H. Ojima, K. Takayama, Y. Tamakawa, T. Yanagisawa, A. Fujiwara and K. Mitoya, "Dual energy flash x-ray generator," *SPIE*, **2513**, pp. 723-735, 1994.
10. A. Shikoda, E. Sato, M. Sagae, T. Oizumi, Y. Tamakawa and T. Yanagisawa, "Repetitive flash x-ray generator having a high-durability diode driven by a two-cable-type line pulser," *Rev. Sci. Instrum.*, **65**, pp. 850-856, 1994.
11. E. Sato, K. Takahashi, M. Sagae, S. Kimura, T. Oizumi, Y. Hayasi, Y. Tamakawa and T. Yanagisawa, "Sub-kilohertz flash x-ray generator utilizing a glass-enclosed cold-cathode triode," *Med. & Biol. Eng. & Comput.*, **32**, pp. 289-294, 1994.
12. K. Takahashi, E. Sato, M. Sagae, T. Oizumi, Y. Tamakawa and T. Yanagisawa, "Fundamental study on a long-duration flash x-ray generator with a surface-discharge triode," *Jpn. J. Appl. Phys.*, **33**, pp. 4146-4151, 1994.
13. E. Sato, M. Sagae, A. Shikoda, K. Takahashi, T. Oizumi, M. Yamamoto, A. Takabe, K. Sakamaki, Y. Hayasi, H. Ojima, K. Takayama and Y. Tamakawa, "High-speed soft x-ray techniques," *SPIE*, **2869**, pp. 937-955, 1996.
14. E. Sato, Y. Hayasi, E. Tanaka, H. Mori, T. Kawai, T. Usuki, K. Sato, H. Obara, T. Ichimaru, K. Takayama, H. Ido and Y. Tamakawa, "Quasi-monochromatic radiography using a high-intensity quasi-x-ray laser generator," *SPIE*, **4682**, pp. 538-548, 2002.
15. E. Sato, Y. Hayasi, R. Germer, E. Tanaka, H. Mori, T. Kawai, H. Obara, T. Ichimaru, K. Takayama and H. Ido, "Intense characteristic x-ray irradiation from weakly ionized linear plasma and applications," *Jpn. J. Med. Imag. Inform. Sci.*, **20**, pp.



148-155, 2003.

16. E. Sato, Y. Hayasi, R. Germer, E. Tanaka, H. Mori, T. Kawai, H. Obara, T. Ichimaru, K. Takayama and H. Ido, "Irradiation of intense characteristic x-rays from weakly ionized linear molybdenum plasma," *Jpn. J. Med. Phys.*, **23**, pp. 123-131, 2003.

17. E. Sato, Y. Hayasi, R. Germer, E. Tanaka, H. Mori, T. Kawai, T. Ichimaru, K. Takayama and H. Ido, "Quasi-monochromatic flash x-ray generator utilizing weakly ionized linear copper plasma," *Rev. Sci. Instrum.*, **74**, pp. 5236-5240, 2003.

18. E. Sato, Y. Hayasi, R. Germer, E. Tanaka, H. Mori, T. Kawai, T. Ichimaru, S. Sato, K. Takayama and H. Ido, "Sharp characteristic x-ray irradiation from weakly ionized linear plasma," *J. Electron Spectroscopy and Related Phenomena*, **137-140**, pp. 713-720, 2004.

19. E. Sato, K. Sato and Y. Tamakawa, "Film-less computed radiography system for high-speed Imaging," *Ann. Rep. Iwate Med. Univ. Sch. Lib. Arts and Sci.*, **35**, pp. 13-23, 2000.

\*dresato@iwate-med.ac.jp; phone +81-19-651-5111; fax +81-19-654-9282

## Quasi-Monochromatic Flash X-Ray Generator Utilizing Disk-Cathode Molybdenum Tube

Eiichi SATO, Michiaki SAGAE, Etsuro TANAKA<sup>1</sup>, Yasuomi HAYASI, Rudolf GERMER<sup>2</sup>, Hidezo MORI<sup>3</sup>, Toshiaki KAWAI<sup>4</sup>, Toshio ICHIMARU<sup>5</sup>, Shigehiro SATO<sup>6</sup>, Kazuyoshi TAKAYAMA<sup>7</sup> and Hideaki IDO<sup>8</sup>

Department of Physics, Iwate Medical University, 3-16-1 Honchodori, Morioka 020-0015, Japan

<sup>1</sup>Department of Nutritional Science, Faculty of Applied Bio-science, Tokyo University of Agriculture, 1-1-1 Sakuragaoka, Setagaya-ku 156-8502, Japan

<sup>2</sup>ITP, FHTW FB1 and TU-Berlin, Blankenhainer Str. 9, D 12249 Berlin, Germany

<sup>3</sup>Department of Cardiac Physiology, National Cardiovascular Center Research Institute, 5-7-1 Fujishiro-dai, Suita, Osaka 565-8565, Japan

<sup>4</sup>Electron Tube Division #2, Hamamatsu Photonics Inc., 314-5 Shimokanzo, Toyooka Village, Iwata-gun 438-0193, Japan

<sup>5</sup>Department of Radiological Technology, School of Health Sciences, Hirosaki University, 66-1 Honcho, Hirosaki 036-8564, Japan

<sup>6</sup>Department of Microbiology, School of Medicine, Iwate Medical University, 19-1 Uchimarui, Morioka 020-8505, Japan

<sup>7</sup>Shock Wave Research Center, Institute of Fluid Science, Tohoku University, 2-1-1 Katahira, Aoba-ku, Sendai 980-8577, Japan

<sup>8</sup>Department of Applied Physics and Informatics, Faculty of Engineering, Tohoku Gakuin University, 1-13-1 Chuo, Tagajo 985-8537, Japan

(Received April 2, 2004; accepted June 14, 2004; published October 8, 2004)

High-voltage condensers in a polarity-inversion two-stage Marx surge generator are charged from  $-40$  to  $-60$  kV using a power supply, and the electric charges in the condensers are discharged to an X-ray tube after closing the gap switches in the surge generator using a trigger device. The X-ray tube is a demountable diode, and the turbomolecular pump evacuates air from the tube with a pressure of approximately 1 mPa. Sharp K-series characteristic X-rays of molybdenum are produced without using a monochromatic filter, since the tube utilizes a disk cathode and a rod target, and bremsstrahlung rays are not emitted in the opposite direction to that of electron acceleration. The peak tube voltage increased with increasing charging voltage and increasing space between the target and cathode electrodes. At a charging voltage of  $-60$  kV and a target-cathode space of 1.0 mm, the peak tube voltage and current were 110 kV and 0.75 kA, respectively. The pulse width ranged from 40 to 100 ns, and the maximum dimension of the X-ray source was 3.0 mm in diameter. The number of generator-produced K photons was approximately  $7 \times 10^{14}$  photons/cm<sup>2</sup>·s at 0.5 m from the source. [DOI: 10.1143/JJAP.43.7324]

KEYWORDS: flash X-ray, characteristic X-ray, quasi-monochromatic radiography, bremsstrahlung X-ray distribution

### 1. Introduction

Flash X-ray generators have been developed as a powerful tool in high-speed radiography because they produce extremely short X-ray pulses of less than 1  $\mu$ s. Currently, most generators utilize a multistage Marx surge generator<sup>1,2)</sup> in order to produce high-photon-energy flash X-rays by increasing the maximum tube voltage. On the other hand, soft flash X-ray generators<sup>3-7)</sup> with photon energies of less than 150 keV can be applied to biomedicine, and the repetition rate has been increased to the sub-kilohertz order.<sup>8)</sup>

High-dose-rate monochromatic X-rays are produced by a synchrotron in conjunction with single crystals and have been applied to X-ray phase imaging<sup>9,10)</sup> and microangiography.<sup>11)</sup> Subsequently, because extremely high-dose-rate quasi-monochromatic X-rays are produced from the axial direction of weakly ionized linear plasma,<sup>12-14)</sup> high-speed biomedical radiography has been performed. However, the bremsstrahlung X-rays are produced using targets of molybdenum, silver, cerium, and tungsten, since high-photon-energy bremsstrahlung X-rays are not absorbed effectively in the linear plasma. In addition, in cases where cold cathode triodes are employed, it is difficult to increase the condenser charging voltage to increase the photon energies of characteristic X-rays due to vacuum breakdown; the target voltage is equal to the charging voltage.

Because bremsstrahlung X-ray intensity varies with changes in the angle and direction of electron acceleration, characteristic X-rays are produced without using a monochromatic filter by selecting the irradiation direction. Although bremsstrahlung intensity is proportional to the atomic number, the angle selection will be a useful technique to produce quasi-monochromatic X-rays.

In this article, we describe a compact flash X-ray

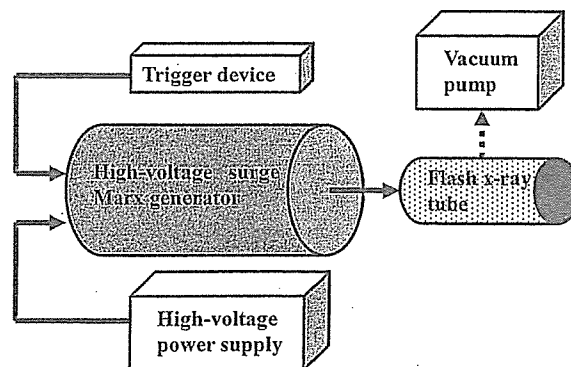


Fig. 1. Block diagram of compact quasi-monochromatic flash X-ray generator:

generator utilizing a molybdenum-target radiation tube, used to perform a preliminary experiment for generating quasi-monochromatic X-rays using the angle dependence of bremsstrahlung rays.

### 2. Generator

#### 2.1 High-voltage circuit

Figure 1 shows a block diagram of a compact quasi-monochromatic flash X-ray generator. This generator consists of the following components: a constant high-voltage power supply, a polarity-inversion two-stage surge Marx generator with a capacity during main discharge of 425 pF, a trigger device for the surge generator, a turbomolecular pump, and a flash X-ray tube. Since the electric circuit of the surge generator employs a polarity-inversion two-stage Marx line (Fig. 2), the surge produces twice the potential of the condenser charging voltage. When two condensers inside of the surge generator are charged from  $-40$  to

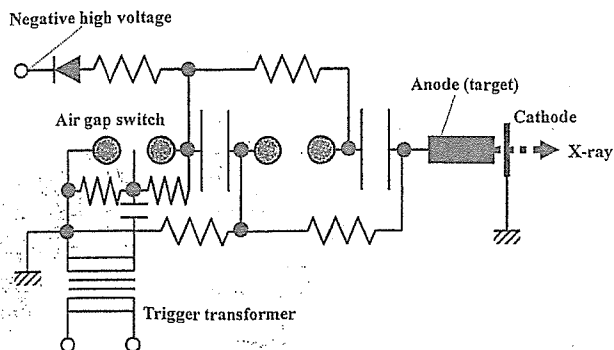


Fig. 2. Circuit diagram of flash X-ray generator.

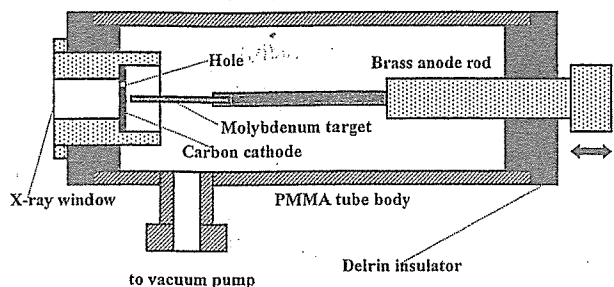


Fig. 3. Schematic drawing of flash X-ray tube.

-60 kV, the ideal output voltage ranges from 80 to 120 kV.

2.2 X-ray tube

The X-ray tube is of the demountable diode type, as illustrated in Fig. 3. This tube is connected to the turbomolecular pump with a pressure of approximately 1 mPa and consists of the following major devices: a rod-shaped molybdenum target, a disk cathode made of graphite, a polyethylene terephthalate (Mylar) X-ray window 0.25 mm in thickness, and a polymethyl methacrylate (PMMA) tube body. The target-cathode (T-C) space was regulated from the outside of the X-ray tube by rotating the anode rod, and

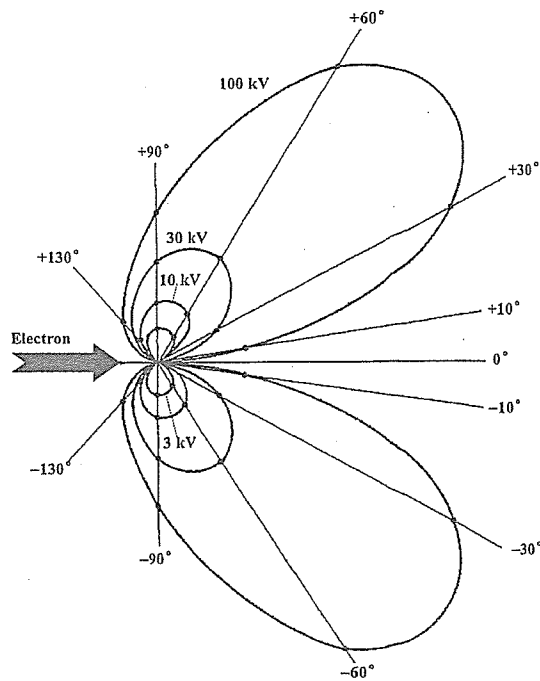


Fig. 4. Bremsstrahlung X-ray intensity distribution vs angle.

the transmission X-rays are obtained through a 1.0 mm-thick graphite cathode and an X-ray window. Because bremsstrahlung rays are not emitted in the opposite direction to that of electron acceleration (Fig. 4), characteristic X-rays can be produced.

3. Characteristics

3.1 Tube voltage and current

Tube voltage and current were measured using a high-voltage divider with an input impedance of 10 kΩ and a current transformer, respectively (Figs. 5 and 6). The voltage and current roughly displayed damped oscillations. At a constant T-C space of 1.0 mm, peak voltage increased slightly with increasing charging voltage. In contrast, peak

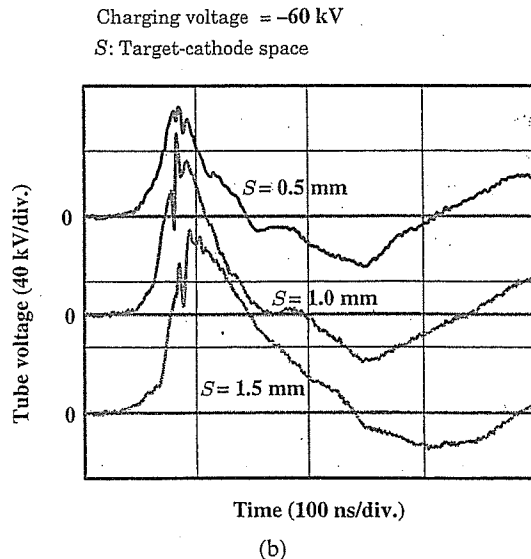
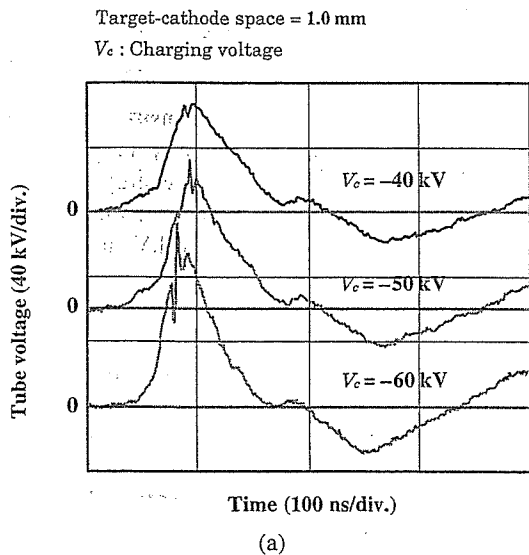


Fig. 5. Variations in tube voltage with changes in (a) charging voltage and (b) space.

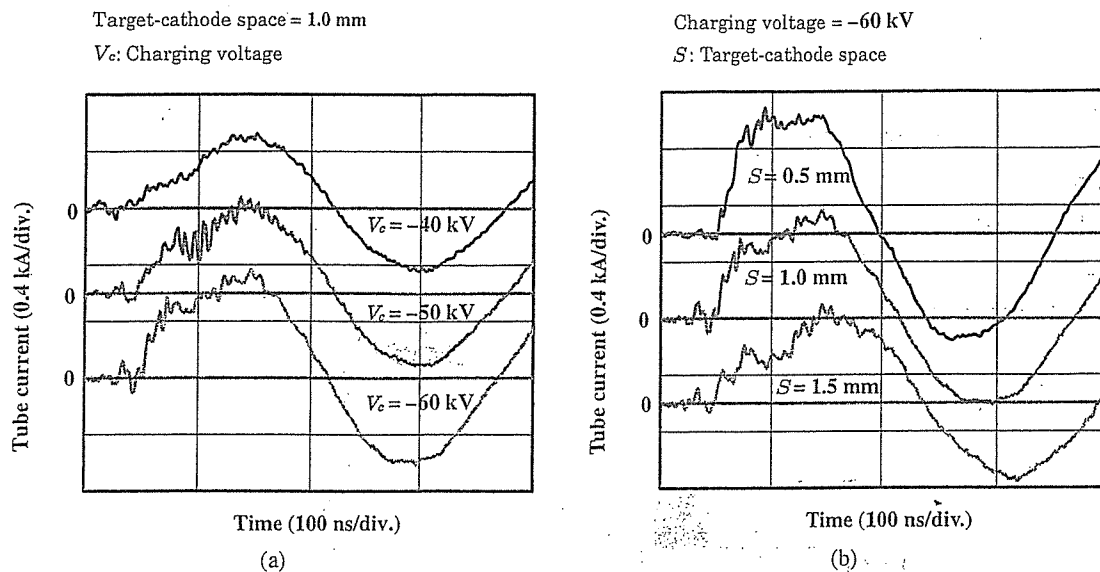


Fig. 6. Tube currents with changes in (a) charging voltage and (b) space.

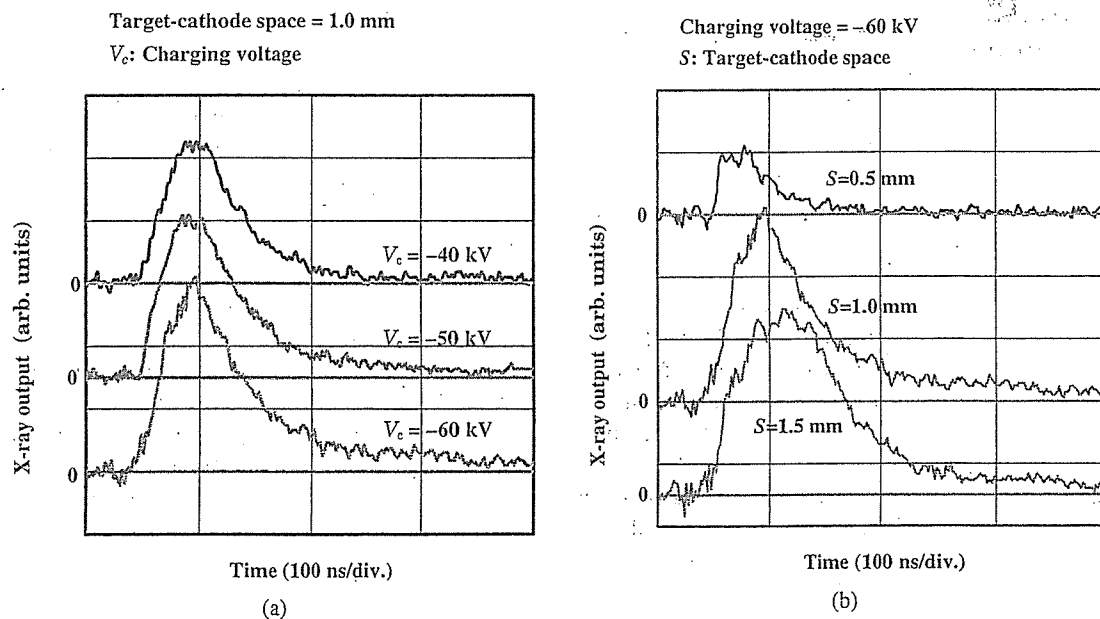


Fig. 7. X-ray outputs according to changes in (a) charging voltage and (b) space.

voltage substantially increased when T-C space was increased at a constant charging voltage of  $-60$  kV. Subsequently, peak tube current increased with increasing charging voltage. When T-C space was increased, current rise time increased, and peak current decreased. At a charging voltage of  $-60$  kV and a T-C space of  $1.0$  mm, peak tube voltage and current were  $110$  kV and  $0.75$  kA, respectively.

### 3.2 X-ray output

X-ray output pulse was detected using a combination of a plastic scintillator and a photomultiplier (Fig. 7). When the charging voltage was increased, the pulse height increased, but the width seldom varied. Next, with increases in the T-C space, the height was maximized, and the width increased. In the present work, the width ranged from  $40$  to  $100$  ns. Next,

the time-integrated X-ray intensity measured using a thermoluminescence dosimeter (Kyokko TLD Reader 1500 having MSO-S elements without energy compensation) was approximately  $3.0 \mu\text{C}/\text{kg}$  at  $0.5$  m from the X-ray source with a charging voltage of  $-60$  kV and a T-C space of  $1.0$  mm.

### 3.3 X-ray source

In order to measure the images of the X-ray source, we employed a pinhole camera with a hole diameter of  $100 \mu\text{m}$  (Fig. 8). When the charging voltage was increased, the plasma X-ray source grew, and both spot dimension and intensity increased. The maximum dimension was almost equal to the target diameter and had a value of approximately  $3.0$  mm.